International Journal on Magnetic Particle Imaging
Vol 10, No 1, Suppl 1, Article ID 2403042, 4 Pages

Infinite Science Publishing

Proceedings Article

A study on different Halbach arrays of magnets in relation to magnetic field gradients in a handheld MPI system

Yang Jing[a,b] · Bo Zhang[a,b] · Yu An[a,b] · Hui Hui[c,*] · Zhenchao Tang[a,b,*] · Jie Tian[a,b,*]

[a] Beijing Advanced Innovation Center for Big Data-Based Precision Medicine, School of Engineering Medicine, Beihang University, Beijing, China
[b] Key Laboratory of Big Data-Based Precision Medicine (Beihang University), Ministry of Industry and Information Technology of the People's Republic of China, Beijing, 100191, China
[c] CAS Key Laboratory of Molecular Imaging, Institute of Automation, Chinese Academy of Sciences, Beijing, China
*Corresponding authors, email: tian@ieee.org, tangzhenchao@buaa.edu.cn, hui.hui@ia.ac.cn

Abstract

Handheld MPI devices have promising clinical application prospects due to their portability. However, there is a lack of detailed analysis of Halbach magnet arrays, which are critical for generating field-free regions in handheld MPI system imaging. Therefore, investigating the relationship between the Halbach array configuration and the resulting magnetic field is necessary. In this study, we modify deformation angle of the magnet, magnet magnetization direction, magnet thickness, and magnet outer radius of cylindrical magnets to vary the Halbach array configuration, and further exploration confirmed their relationship with the magnetic field gradients. In the future, these results can be used as reference to adjust the configuration of the Halbach magnet array to better meet clinical requirements, which might further promote the application of handheld MPI.

I. Introduction

Magnetic particle imaging (MPI) is a novel functional imaging technique that utilizes the nonlinear magnetic response of magnetic nanoparticles (MNPs) for tomographic imaging [1]. The technique has promising applications in various fields such as cell tracking, inflammation imaging, vascular imaging and cancer diagnosis [2]. Among the various MPI devices, handheld MPI scanners have the advantage of being small and portable, allowing physicians to reach out to the lesion site for detection or imaging, thus providing greater flexibility compared to fixed structures [3], [4].

To ensure the mobility of handheld MPI devices, the number of magnets is limited, nevertheless which also results in poor magnetic field gradients. There have been many previous studies using Halbach array-based rings for generating magnetic field-free regions [5], [6], [7], which have performed well in generating magnetic fields, showing the potential of Halbach arrays in the development of handheld MPI.

In this study, we hope to improve the magnetic field gradient and reduce the size of FFP by investigating the effects of magnet deformation angle, magnet magnetization direction, magnet thickness and outer radius on the magnetic field gradient, which might contribute to the imaging of future handheld MPI devices.

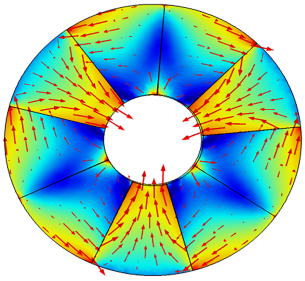

Figure 1: Each sector magnet and its magnetizing direction

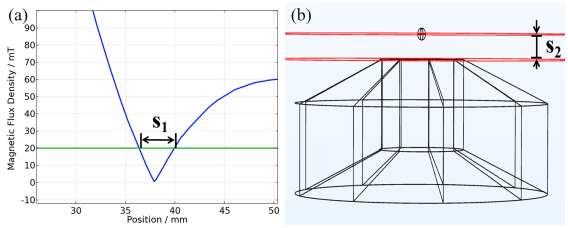

Figure 2: (a) The FFP size(s1) in the simulation results; (b) The detection depth(s2) in the simulation results.

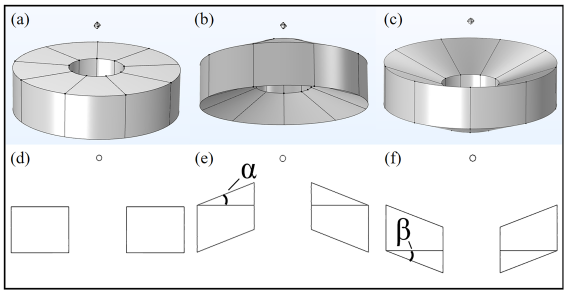

Figure 3: Magnets of the same volume but different shapes. (a) No deformation; (b) The concave side facing FFP; (c) The convex side facing FFP. The small ball at the top of the figures represents FFP. (d), (e) and (f) depict, respectively, cross sections of the above shaped magnets. α and β show the deformation angle of magnets.

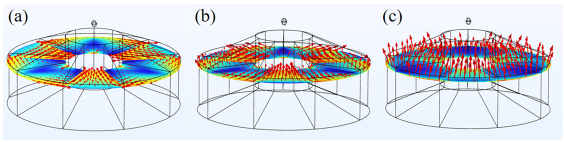

Figure 4: Simulation results for three different magnet magnetization directions. (a), (b) and (c) indicate that the magnet is magnetized at an angle of 0°, 40° and 80°, respectively, to the plane of the figure.

II. Material and methods

II.I. Simulation materials and grids

In this study, COMSOL software was used for simulation. Sintered NdFeB, chosen for its superior magnetic properties and cost-efficiency among permanent magnetic materials, serves as the ideal magnet material. To ensure accuracy, the mesh surrounding the magnet will be finer than the air mesh.

II.II. Experimental method

In this study, in order to place more magnets in the same space, sector magnets were chosen instead of bar magnets to generate the magnetic field gradient. Nine sector magnets were divided into three groups, which together enclosed a hollow cylinder. As in Fig.1, The projections of the magnetization direction on the surface of the cylinder for three of the sector magnets in each group are clockwise, radially inward, and counterclockwise, respectively.

In order to investigate the effect of the Halbach array on the magnetic field gradient field, while keeping the other three parameters unchanged, deformation angle of the magnet, magnet magnetization direction, magnet thickness and magnet outer radius were sequentially changed. Then the size and detection depth of the FFP are calculated based on the COMSOL simulation results. As shown in Fig.2, we define the s_1 as the size of the FFP near the lowest point of the magnetic field that is lower than a specific critical value, and the detection depth (s_2) as the perpendicular distance of the FFP from the closest point of the magnet.

II.III. Magnet Array Settings

For the study of the magnet deformation, as shown in Fig.3, it can be divided into three categories: original hollow cylinder, magnet deformation with the concave side facing FFP, magnet deformation with the convex side facing FFP. For the latter two, we can further change their shapes based on the angles α and β, as shown in Fig.3.

For the study of magnet magnetization direction, due to the reality, it is explored in two cases: firstly, for the case of magnet with no shape change or concave surface facing FFP, sampling points in the angle range of 0-50 degrees are selected for simulation; and secondly, for the case of convex surface facing FFP, sampling points in the angle range of 75 to 90 degrees are selected for simulation. Fig.4 shows the simulation results at different magnetization angles.

For the study of magnet thickness, sampling points are selected in the thickness range of 5 mm to 40 mm. For the study of magnet outer radius, sampling points are selected in the range of 25 mm to 50 mm.

10.18416/ijmpi.2024.2403042

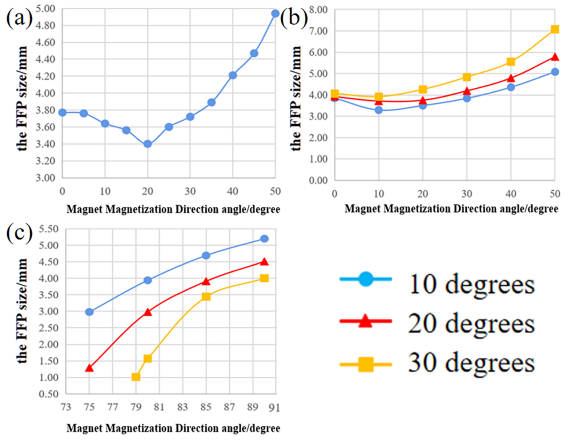

Figure 5: The relationship between the FFP size (s_1) and the magnet magnetization direction. (a), (b) and (c) represent the cases of zero magnet deformation, magnet concave side facing FFP, and magnet convex surface facing FFP, respectively. The legend shows the deformation angle (α or β) of magnet.

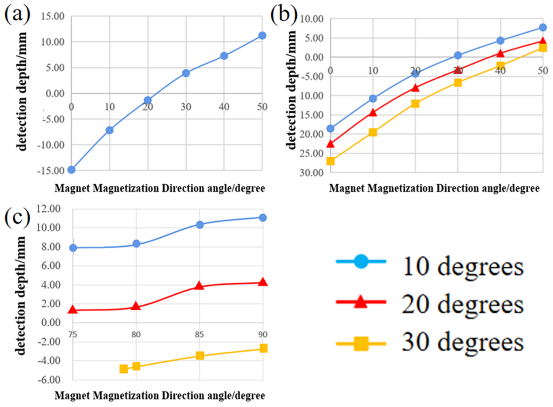

Figure 6: The relationship between the detection depth (s_2) and the magnet magnetization direction. (a), (b) and (c) represent the cases of zero magnet deformation, magnet concave side facing FFP, and magnet convex surface facing FFP, respectively. The legend shows the deformation angle (α or β) of magnet.

III. Results and discussion

III.I. The Influence of Magnet shape and Magnet Magnetization Direction on FFP

As shown in Fig.5, it can be seen that the size of FFP (s_1) is generally positively correlated with the angle of the magnet magnetization direction. As can be seen in Fig.6, the detection depth (s_2) is also positively correlated with the angular magnitude of the magnet magnetization direction.

III.II. The Influence of magnet thickness on FFP

In this part, the shape of the magnet is the original hollow cylinder. The magnet magnetization direction angle, inner radius and outer radius are fixed at 30°, 30 mm and 50 mm respectively, but the magnet thickness can be changed.

It can be observed from Fig.7 that when the magnet thickness is less than a certain value, the FFP size (s_1) decreases with the increase of the magnet thickness, nevertheless when the magnet thickness reaches a certain value and then increases, the FFP size (s_1) stabilizes around a fixed value.

It can be inferred from the simulation results in Fig.8 that the detection depth (s_2) is negatively correlated with the thickness of the magnet.

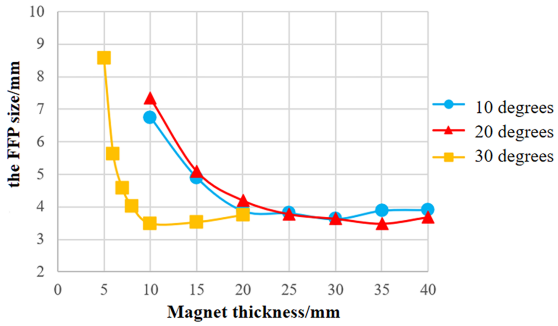

Figure 7: The relationship between FFP size (s1) and magnet thickness. Three curves represent the angle of magnet magnetization direction is 10, 20 and 30 degrees, respectively.

III.III. The Influence of magnet outer radius

In this part, the shape of the magnet is the original hollow cylinder. The magnet magnetization direction angle, inner radius and thickness are fixed at 30°, 30 mm and 30 mm respectively, but the magnet outer radius can be changed.

From Fig.9, it can be seen that when the outer radius of the magnet is small, the FFP size (s_1) decreases with the increase of the outer radius. However, when the outer radius reaches a certain value and then increase, the FFP size stabilizes around a fixed value.

As shown in Fig.10, there is a positive correlation between detection depth (s_2) and the magnet outer radius, which means that the generated FFP position is further away from the magnet when the magnet outer radius increases.

10.18416/ijmpi.2024.2403042

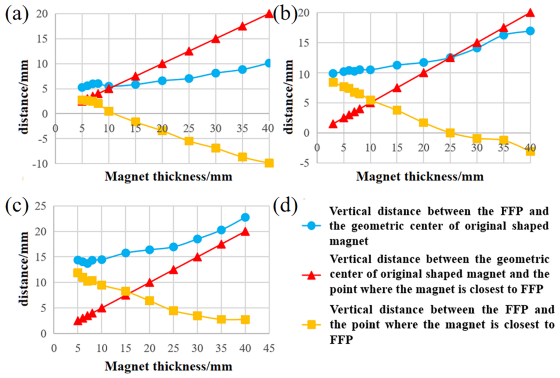

Figure 8: The relationship between the detection depth (s2) and the magnet thickness. The value corresponding to the yellow curve is equal to the blue curve minus the red curve. (a), (b) and (c) represent the cases when the angle of magnet magnetization direction is 10, 20 and 30 degrees, respectively. (d) is the corresponding legend.

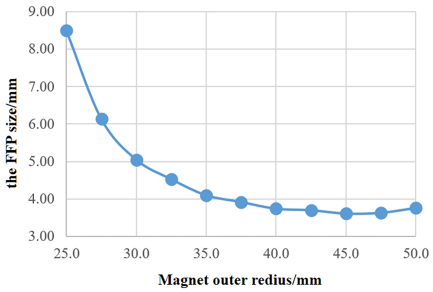

Figure 9: The relationship between FFP size (s_1) and the magnet outer radius.

IV. Conclusions

In this study, we further explore the influence of different Halbach arrays on the magnetic field gradients. The results show that by changing deformation angle, magnetization direction, thickness, and outer radius of the cylindrical magnet, the generated magnetic field will change according to a certain pattern. In the future, based on this, the quantitative relationship between the configuration of the Halbach magnet array and the magnetic field gradient can be obtained through data fitting. Combined with clinical practice, it is expected to improve the imaging ability of handheld MPI.

Acknowledgments

This paper is supported by the National Natural Science Foundation of China under Grant No. 62027901, 81771806, 61936013, 81871511; Young Elite Scientists Sponsorship Program by CAST (2023QNRC001); the Beijing Natural Science Foundation under Grant No. 7212051; National Key R&D Program of China, 2021YFA1301603; Key-Area Research and Development Program of Guangdong Province (2021B0101420005).

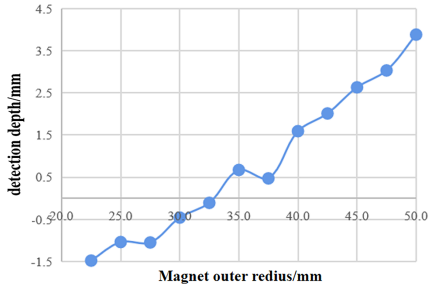

Figure 10: The relationship between the detection depth (s_2) and the magnet outer radius.

Author's statement

Conflict of interest: Authors state no conflict of interest.

References

[1] Gleich B, Weizenecker J. Tomographic imaging using the nonlinear response of magnetic particles[J]. Nature, 2005, 435(7046): 1214-1217.

[2] Talebloo N, Gudi M, Robertson N, et al. Magnetic particle imaging: current applications in biomedical research[J]. Journal of Magnetic Resonance Imaging, 2020, 51(6): 1659-1668.

[3] Choi S H, Le T A, Son B, et al. A portable single-sided magnetic particle imaging concept using amplitude modulation for breast conserving sugery[J]. International Journal on Magnetic Particle Imaging IJMPI, 2022, 8(1 Suppl 1).

[4] Mason E E, Mattingly E, Herb K, et al. Concept for using magnetic particle imaging for intraoperative margin analysis in breast-conserving surgery[J]. Scientific Reports, 2021, 11(1): 13456.

[5] Weber M, Beuke J, von Gladiss A, et al. Novel field geometry using two Halbach cylinders for FFL-MPI[J]. International Journal on Magnetic Particle Imaging, 2018, 4(2): 2019.

[6] Vogel P, Markert J, Rückert M A, et al. Magnetic particle imaging meets computed tomography: First simultaneous imaging[J]. Scientific reports, 2019, 9(1): 12627.

[7] Wang Q, Zhang Z, Xu C, et al. Single-sided magnetic particle imaging devices using ferrite core to improve penetration depth[J]. International Journal on Magnetic Particle Imaging IJMPI, 2023, 9(1 Suppl 1).

